Electronic Supporting Information (ESI)

Two robust metal-organic frameworks with uncoordinated N atoms for CO_2 adsorption

Guo-Jian Ren, Yan-Qing Liu, Tong-Liang Hu* and Xian-He Bu

School of Materials Science and Engineering, National Institute for Advanced Materials, Collaborative Innovation Center of Chemical Science and Engineering(Tianjin), Nankai University, Tianjin 300071, P. R. China.

* Corresponding author. E-mail: tlhu@nankai.edu.cn

CONTENTS

S1. Materials and general methods

All the chemicals used for synthesis were of analytical grade and commercially available. IR spectra were measured on a Tensor 27 OPUS (Bruker) FT-IR spectrometer with KBr pellets. Powder X-ray diffraction (PXRD) spectra were recorded on a Rigaku D/Max-2500 diffractometer at 40 kV, 100 mA for a Cu-target tube and a graphite monochromator. Thermogravimetric analyses (TGA) were carried out on a Rigaku standard TG-DTA analyzer under N_2 with a heating rate of 10 °C min^{-1}, with an empty Al_2O_3 crucible used as reference. Simulation of the PXRD pattern was carried out by the single-crystal data and diffraction-crystal module of the Mercury (Hg) program version 3.0 available free of charge via the Internet at http://www.iucr.org. Magnetic measurements were carried out using a Magnetic Property Measurement System (MPMS3).

S2. Adsorption measurements

Low pressure gas adsorption measurements were performed using an ASAP 2020 M gas adsorption analyzer. Prior to measurement, the fresh samples were soaked in absolute ethanol to exchange the occluded solvent for 48 h. Then the processed samples were loaded in sample tubes and activated under high vacuum (less than 10^{-5} Torr) at 120 °C. Degassed samples were used for gas sorption measurements. The N_2 sorption isotherms were collected at 77 K in a liquid nitrogen bath. The CO_2 adsorption isotherms were collected at 273 K in an ice water mixture bath, and as the center-controlled air conditioner was set up at 25 and 50 ^{o}C, a water bath was used for adsorption isotherms at 298 and 323 K. High-pressure gas adsorptions were performed with a Hiden Isochema Intelligent Gravimetric Analyser (IGA-100B). The pre-treatment of the fresh samples was the same with the low pressure measurement, and then the processed samples were loaded in sample basket and degassed under high vacuum.

The virial equation was used to fit the combined CO_2 isotherm data for **1** and **2** at 273 K, 298 K and 323 K.[1-2]

S3. Crystal structure determination

Single crystal X-ray diffraction measurement was carried out on Rigaku Saturn70 diffractometer at 113.15 K for the title compounds with Mo-Kα radiation (λ = 0.71075 Å). The program CrystalClear was used for the integration of the diffraction profiles. The structures were solved by direct methods using the SHELXS program of the SHELXTL package and refined with SHELXL.[3] It should be noted that the guest molecules in the complexes are highly disordered and could not be modeled properly, so the diffused electron densities resulting from them were removed by the SQUEEZE routine in PLATON[4] and the results were appended in the CIF files. During the refinements of (1) and (2) it became clear that the crystals of the two isomorphous compounds were of opposite chirality as shown by the Flack values [0.92(4) for (1) and 0.011(8) for (2)]. Accordingly, for publication purposes the structure of (1) was inverted and the refinement redone leading to a Flack value of 0.08(4).

S4. Bond valence sum (BVS)

The valence of a bond between two atoms, i and j is given by S_{ij}. The sum of S_{ij} is the valence of the i atom. The calculated results are shown in the following tables.[5,6]

Table S1. BVS for Co^{2+} and μ_3-oxygen atom in **1**.

Co^{2+}	r_0	r_{ij}	B	$S_{ij}=\exp[(r_0-r_{ij})/B]$
Co(1)-O(2)	1.685	2.038	0.37	0.3856
Co(1)-O(1)	1.685	2.119	0.37	0.3094
Co(1)-O(1)#1	1.685	2.119	0.37	0.3094
Co(1)-N(1)	1.650	2.117	0.37	0.2730
Co(1)-N(2)	1.650	2.156	0.37	0.2547
Co(1)-N(2) #1	1.650	2.156	0.37	0.2547

$V_{Co1} = \Sigma S_{ij} = 1.797$ $V_{O2} = 3\times S_{Co1\text{-}O2} = 1.157$

Table S2. BVS for Co^{3+} and μ_3-oxygen atom in **1**.

Co^{3+}	r_0	r_{ij}	B	$S_{ij}=\exp[(r_0-r_{ij})/B]$

Co(1)-O(2)	1.637	2.038	0.37	0.3387
Co(1)-O(1)	1.637	2.119	0.37	0.2718
Co(1)-O(1)#1	1.637	2.119	0.37	0.2718
Co(1)-N(1)	1.750	2.117	0.37	0.3709
Co(1)-N(2)	1.750	2.156	0.37	0.3338
Co(1)-N(2) #1	1.750	2.156	0.37	0.3338

$V_{Co1} = \Sigma S_{ij} = 1.921$ $V_{O2} = 3\times S_{Co1\text{-}O2} = 1.016$

Table S3. BVS for Ni^{2+} and μ_3-oxygen atom in **2**.

Ni^{2+}	r_0	r_{ij}	B	$S_{ij}=\exp[(r_0-r_{ij})/B]$
Ni(1)-O(2)	1.670	1.995	0.37	0.4150
Ni(1)-O(1)	1.670	2.073	0.37	0.3365
Ni(1)-O(1)	1.670	2.073	0.37	0.3365
Ni(1)-N(3)	1.647	2.070	0.37	0.3188
Ni(1)-N(1)	16.47	2.083	0.37	0.3078
Ni(1)-N(1)	1.647	2.083	0.37	0.3078

$V_{Ni1} = \Sigma S_{ij} = 2.022$ $V_{O2} = 3\times S_{Ni1\text{-}O2} = 1.245$

Table S4. BVS for Ni^{3+} and μ_3-oxygen atom in **2**.

Ni^{3+}	r_0	r_{ij}	B	$S_{ij}=\exp[(r_0-r_{ij})/B]$
Ni(1)-O(2)	1.750	1.995	0.37	0.5174
Ni(1)-O(1)	1.750	2.073	0.37	0.4654
Ni(1)-O(1)	1.750	2.073	0.37	0.4654
Ni(1)-N(3)	1.731	2.070	0.37	0.4579
Ni(1)-N(1)	1.731	2.083	0.37	0.4579
Ni(1)-N(1)	1.731	2.083	0.37	0.3719

$V_{Ni1} = \Sigma S_{ij} = 2.523$ $V_{O2} = 3\times S_{Ni1\text{-}O2} = 1.546$

S5 Magnetic measurement

Magnetic measurements are performed in order to determine the oxidation states of the metal ions. The data is corrected for the diamagnetism, and then fitted to the Curie-Weiss law in the temperature range 50-300 K for **1**. The obtained experimental value C_{exp} of 10.10 $\mathrm{cm^3\ K\ mol^{-1}}$ as well as $\chi_{\mathrm{m}}T$ product (7.94 $\mathrm{cm^3\ K\ mol^{-1}}$) at 300 K displays consistence with the reported result, corresponding to the presence of 3 $\mathrm{Co^{2+}}$ ($S = 3/2$).[7]

As for **2**, the data is corrected for the diamagnetism, and then fitted to the Curie-Weiss law in the temperature range 50-300 K. The obtained experimental value C_{exp} of 2.69 $\mathrm{cm^3\ K\ mol^{-1}}$ fits well to the Curie constant of 2.38 corresponding to the presence of 2 $\mathrm{Ni^{2+}}$ ($S = 1$) and 1 low spin $\mathrm{Ni^{3+}}$ ($S = 1/2$) per formula unit.[5,6]

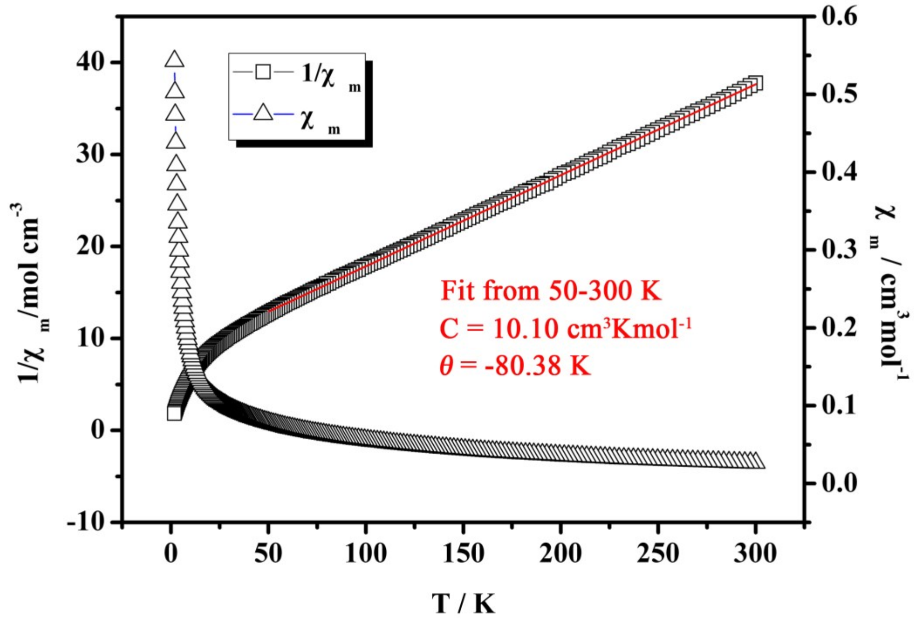

Fig. S1 Plots of χ_{m} versus T (triangle), $1/\chi_{\mathrm{m}}$ versus T (square) and linear fitting to the Curie-Weiss law (red) for after-activated sample of **1**.

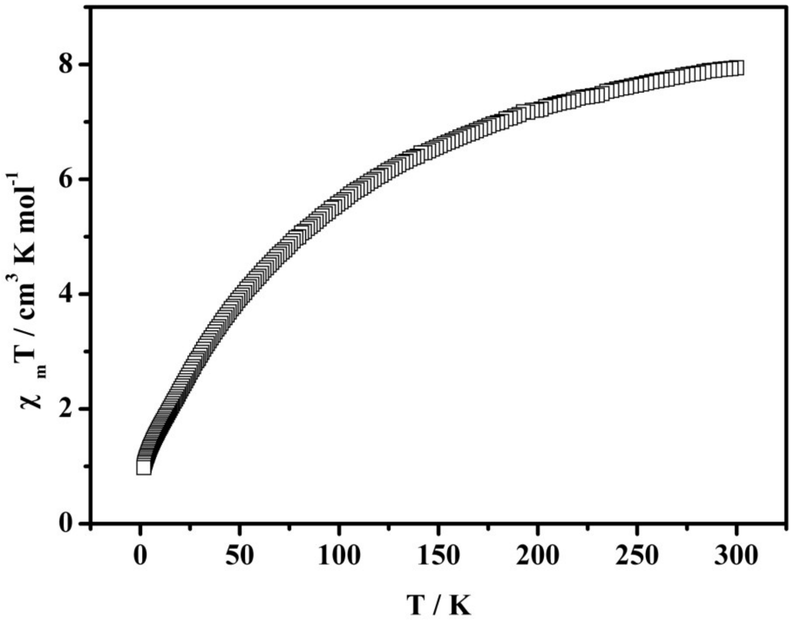

Fig. S2 Plot of $\chi_M T$ vs T for **1**.

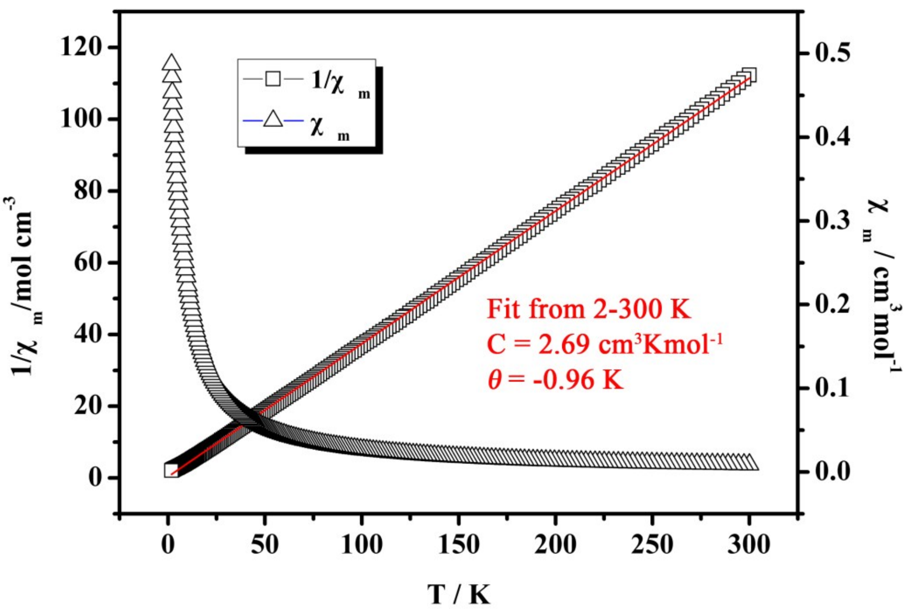

Fig. S3 Plots of χ_m versus T (triangle), 1/χ_m versus T (square) and linear fitting to the Curie-Weiss law (red) for after-activated sample of **2**.

S6. Supplementary characterizations, gas adsorptions

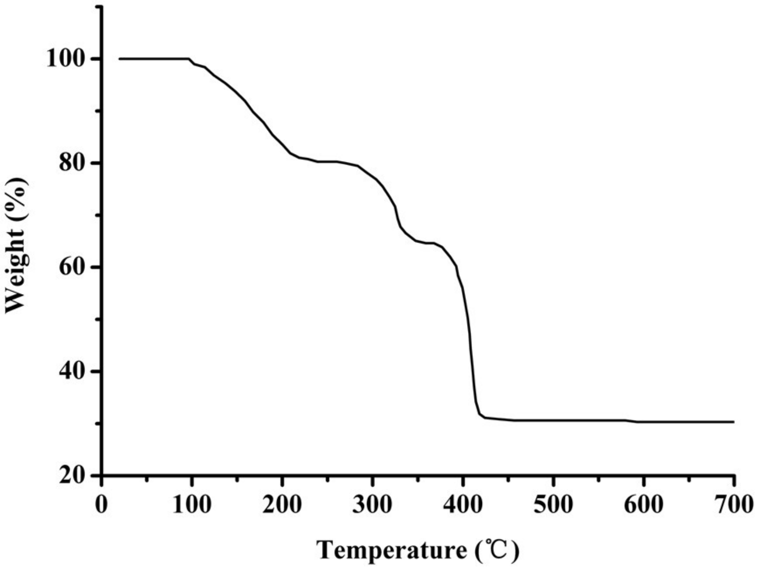

Fig. S4. TGA curve of compound **1**.

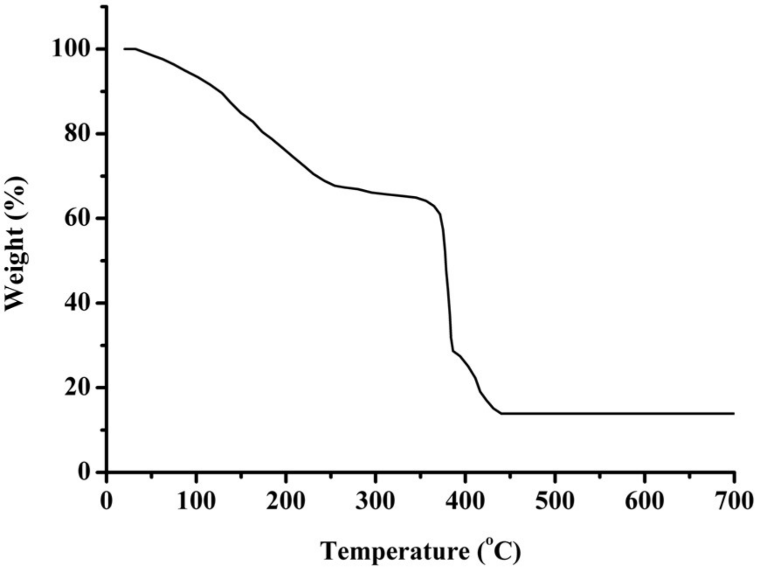

Fig. S5. TGA curve of compound **2**.

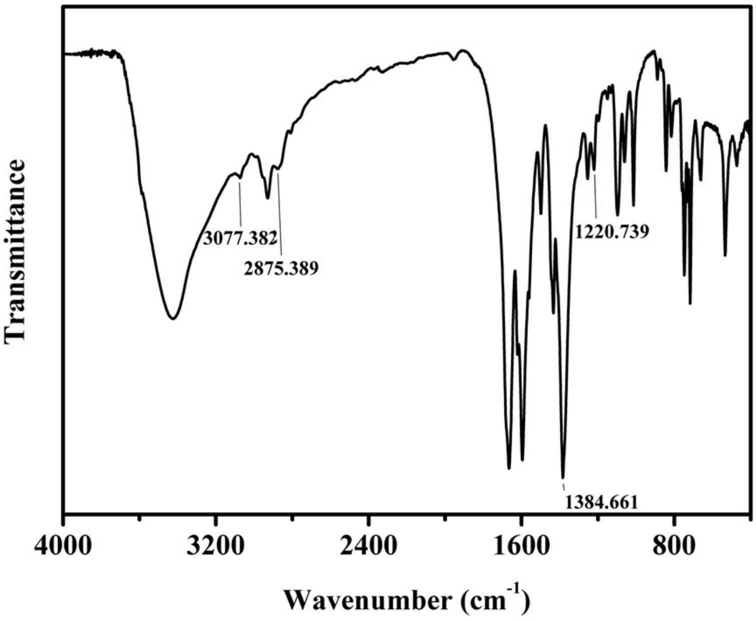

Fig. S6. IR spectrum of compound **1** (the vibration bands around 3077, 2875, 1220 cm^{-1} indicate the presence of dimethylamine cation, and the vibration band of 1384 cm^{-1} can attribute to the NO^{3-}).

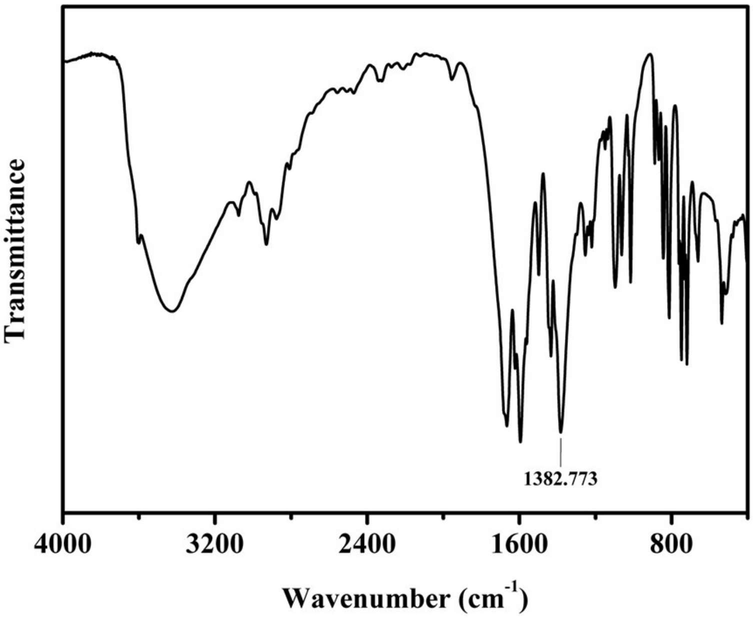

Fig. S7. IR spectrum of compound **2** (the vibration band of 1382 cm^{-1} can attribute to the NO^{3-}).

S7. The topology presentation of complexes

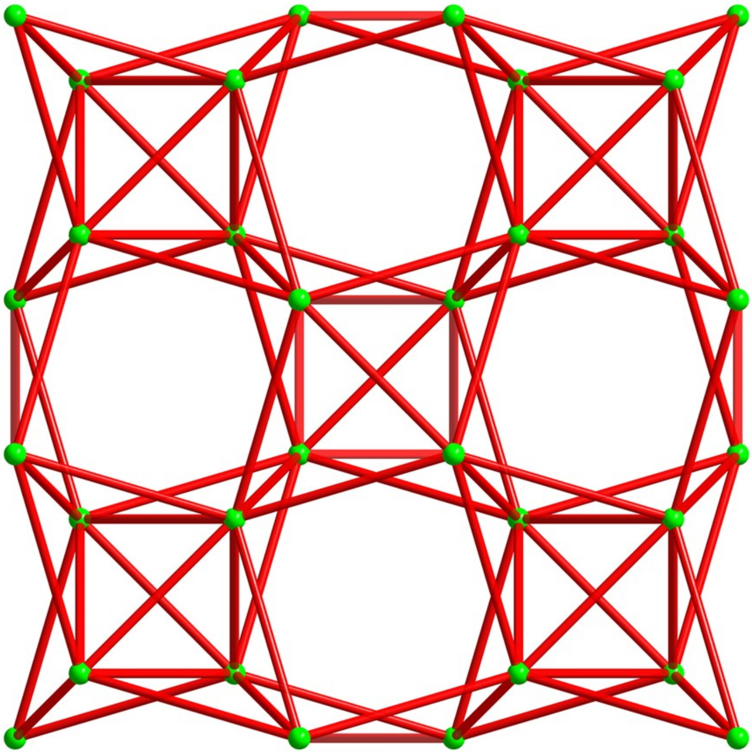

Fig. S8. The topology presentation of complexes **1** and **2**.

S8. The pore size distribution of complexes and estimation of adsorption enthalpies

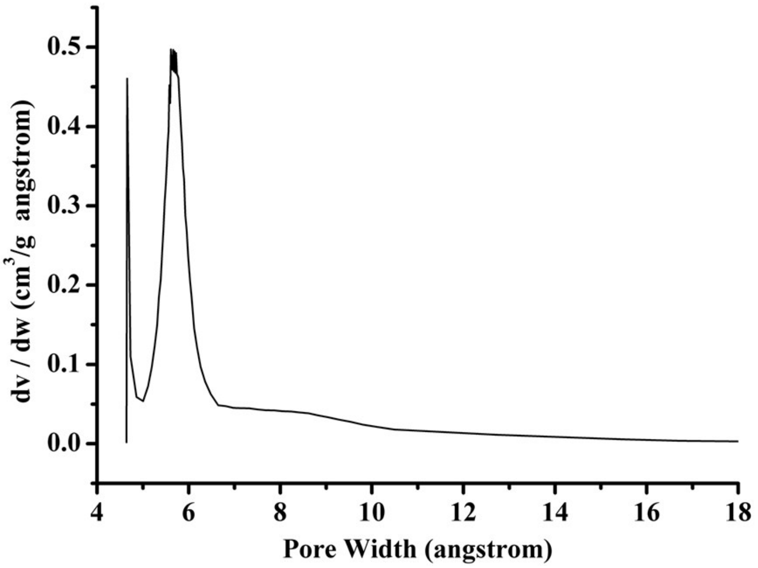

Fig. S9. Horvath-Kawazoe pore size distribution plot of complex **1**.

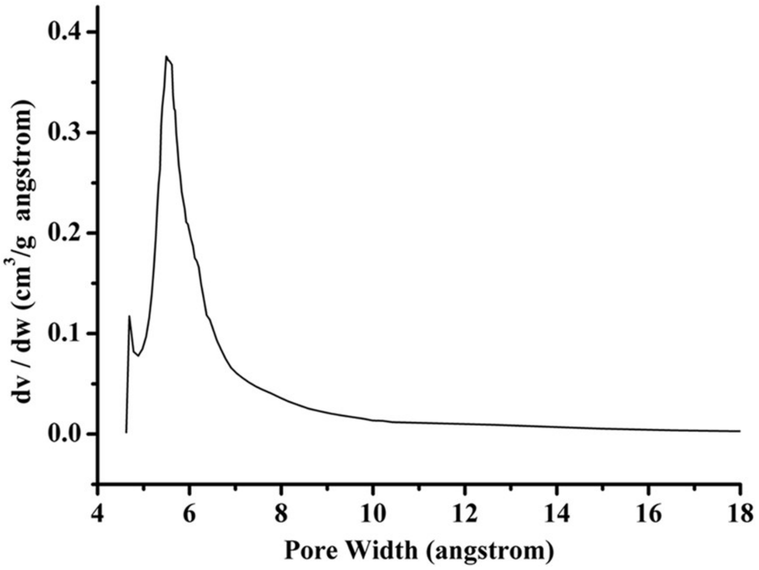

Fig. S10. Horvath-Kawazoe pore size distribution plot of complex **2**.

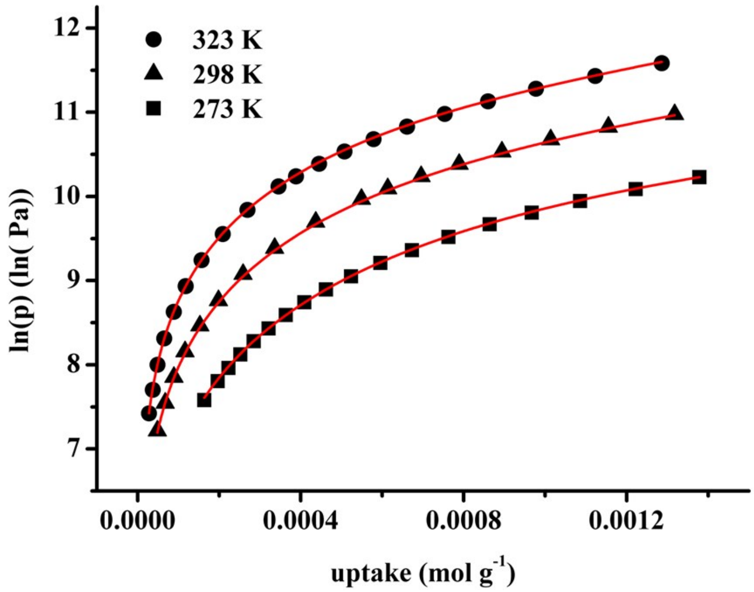

Fig. S11 CO_2 adsorption isotherms for **1**, and the respective virial fits (red lines).

Fit parameters

a0	a1	a2	a3
-3148.8	1.2E6	-7.6E8	2.15E11
a4	b0	b1	b2
-4.5E13	27.6	-2838.6	1.3E6

Adj. R-Square = 0.99981

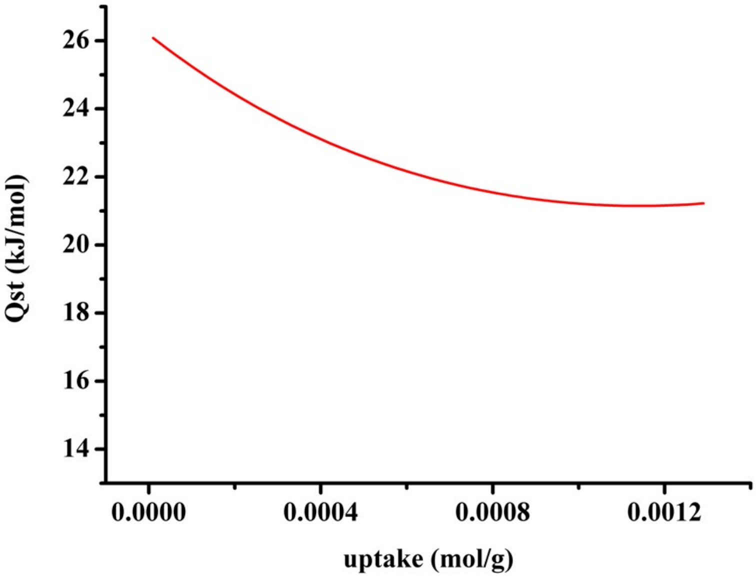

Fig. S12 Adsorption heat of complex **1**.

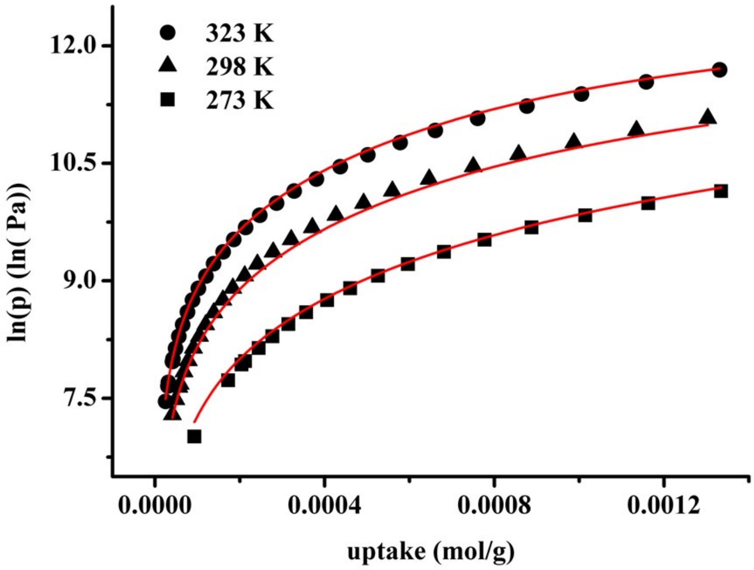

Fig. S13 CO_2 adsorption isotherms for **2**, and the respective virial fits (red lines).

Fit parameters

a0	a1	a2	a3
-2888.8	-97500.3	2.4E8	-8.5E10
a4	b0	b1	b2
3.0E13	27.0	707.7	-750751.4

Adj. R-Square = 0.99613

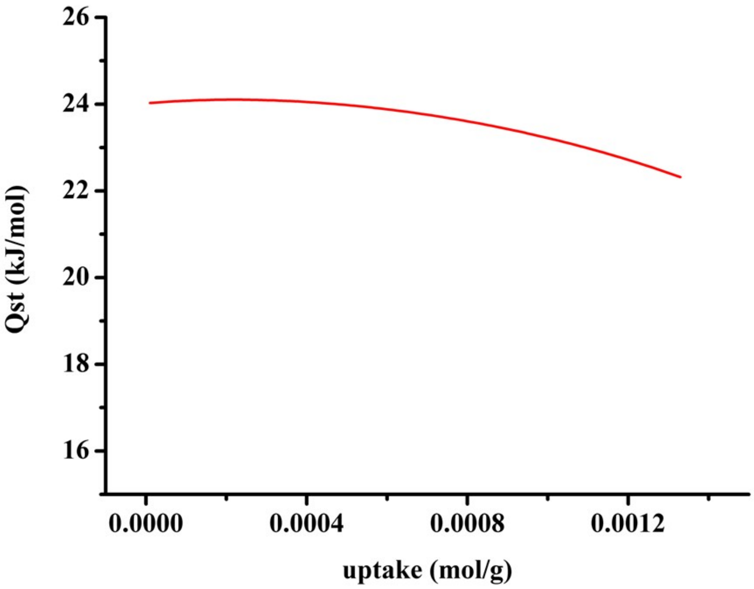

Fig. S14 Adsorption heat of complex **2**.

Reference

1. X. Duan, J. Yu, J. Cai, Y. He, C. Wu, W. Zhou, T. Yildirim, Z. Zhang, S. Xiang, M. O'Keeffe, B. Chen and G. Qian, *Chem. Commun.*, 2013, **49**, 2043-2045.

2. X. Lin, I. Telepeni, A. J. Blake, A. Dailly, C. M. Brown, J. M. Simmons, M. Zoppi, G. S. Walker, K. M. Thomas, T. J. Mays, P. Hubberstey, N. R. Champness and Martin Schröder, *J. Am. Chem. Soc.*, 2009, **131**, 2159-2171.

3. G. M. Sheldrick, *Acta Cryst.* 2015. **C71**, 3-8.

4. A. L. Spek, *J. Appl. Crystallogr.*, 2003, **36**, 7-13.

5. J. H. Jia, X. Lin, C. Wilson, A. J. Blake, N. R. Champness, P. Hubberstey, G. Walker, E. J. Cussen and M. Schröder, *Chem. Commun.*, 2007, 840-842.

6. Y. B. Zhang, W. X. Zhang, F. Y. Feng, J. P. Zhang and X. M. Chen, *Angew. Chem., Int. Ed.*, 2009, **48**, 5287-5290.

7. Q. Chen, J. B. Lin, W. Xue, M. H. Zeng and X. M. Chen, *Inorg. Chem.*, 2011, **50**, 2321-2328.